This is an Accepted Manuscript of an article published by American Physiological Society in Journal of Neuropharmacology.

Final publication is available at
http://jn.physiology.org/content/107/2/649.long

1   Glutamate transporter dysfunction associated with nerve injury-induced pain in mice

2   Ian A Napier, Sarasa A Mohamadi, MacDonald J Christie

3   Discipline of Pharmacology, The University of Sydney, NSW 2006, Australia

4

5

6   **Running Head:** Glutamate transporter dysfunction in neuropathic pain

7

8

9   **Corresponding author:** MJ Christie, Discipline of Pharmacology D06 University of Sydney

10   NSW 2006, Australia. Email: mac.christie@sydney.edu.au. Phone: +61 2 9351 0899, Fax: +61

11   2 9114 4015

12

13

14

15

16   **Abstract**

17   Dysfunction at glutamatergic synapses has been proposed as a mechanism in the

18   development of neuropathic pain. Here we sought to determine whether peripheral nerve

19   injury-induced neuropathic pain results in functional changes to primary afferent synapses.

20   Signs of neuropathic pain as well as an induction of glial fibrillary acidic protein in

21   immunostained spinal cord sections 4 days after partial ligation of the sciatic nerve

22   indicated the induction of neuropathic pain. We found that following nerve injury, no

23   discernable change to kinetics of AMPA or NMDA receptor (NMDAR)-mediated evoked

24   excitatory post synaptic currents (eEPSCs) could be observed in dorsal horn (lamina I/II)

25   neurons compared to those of naive mice. However, we did find that nerve injury was

26   accompanied by slowed decay of the early phase of eEPSCs in the presence of glutamate

27   transporter inhibition by the competitive non-transportable inhibitor DL-threo-β-

28   Benzyloxyaspartic acid (TBOA). Concomitantly, expression patterns for the two major

29   glutamate transporters in spinal cord, EAAT1 and EAAT2, were found to be reduced at this

30   time (4 days post-injury). We then sought to directly determine whether nerve injury results

31   in glutamate spillover to NMDARs at dorsal horn synapses. By employing the use-dependent

32   NMDAR blocker (±)MK-801 to block subsynaptic receptors, we found that although TBOA-

33   induced spillover to extra-synaptic receptors trended to increased activation of these

34   receptors after nerve injury, this was not significant compared to naive mice. Together,

35   these results suggest the development of neuropathic pain involves subtle changes to

36   glutamate transporter expression and function that could contribute to neuropathic pain

37   during excessive synaptic activity.

40   **Introduction**

41   The synaptic mechanisms associated with development of chronic neuropathic pain remain

42   poorly understood (Graham *et al.* 2007). An interplay of both an increase in primary

43   afferent activity or glutamate release, as well as an impairment of glutamate re-uptake at

44   primary afferent synapses in the dorsal horn have been proposed as possible mechanisms

45   for the development of neuropathic pain (Tsuda *et al.* 2005; Sandkuhler 2007; Scholz and

46   Woolf 2007).

47   One of the key components of normal sensory neurotransmission is the tight coupling of

48   excitatory neurotransmitter release with rapid reuptake. Recovery of synaptic glutamate is

49   mediated by a family of specific high-affinity membrane transporters (Danbolt 2001), the

50   excitatory amino acid transporters (EAATs). Astrocytes express two such transporters,

51   EAAT1 (GLAST, Slc1a3) and EAAT2 (GLT-1, Slc1a2), which are together responsible for the

52   majority of synaptic glutamate re-uptake (Rothstein *et al.* 1994; Chaudhry *et al.* 1995;

53   Rothstein *et al.* 1996). A third, neuronal isoform, known as EAAT3 (EAAC1, Slc1a1) is also

54   found in the spinal cord, on primary afferents interneurons and motor neurons of the

55   ventral horn but plays only a limited role in synaptic glutamate re-uptake (Rothstein *et al.*

56   1994; Peghini *et al.* 1997; Stoffel *et al.* 2004; Sun *et al.* 2011). Intrathecal administration of

57   EAAT inhibitors produces pain behaviours suggesting that dysfunction of these transporters

58   may contribute to signs of neuropathic pain (Liaw *et al.* 2005; Weng *et al.* 2006). Findings of

59   pathological changes to astroglia during development of neuropathic pain have raised the

60   possibility that EAAT function may be impaired in the vicinity of primary afferent synapses.

61   Recent reports have indicated that spinal EAAT expression can both increase and decrease

62   in the first 7 days following peripheral nerve injury in rodent neuropathic pain models (Sung

63   *et al.* 2003; Wang *et al.* 2006; Sung *et al.* 2007; Tawfik *et al.* 2008; Xin *et al.* 2009) with

64   substantial losses at day 7 and beyond. It has also been shown that these expression

65   changes coincide with the development of neuropathic pain. However, exactly how these

66   expression changes contribute to altered glutamatergic synaptic transmission has not yet

67   been fully elucidated.

68   The aims of this study were therefore to determine if peripheral nerve injury influences the

69   expression and uptake capacity of spinal glutamate transporters at functioning

70   glutamatergic synapses in spinal cord of nerve injured mice during development of

71   neuropathic pain. Although behavioural signs and markers of neuropathic pain such as

72   astrocyte activation were observed after nerve injury, we found only a modest reduction in

73   glutamate transporter expression after nerve injury and evidence for limited changes to

74   glutamatergic transmission at primary afferent synapses that would be indicative of

75   impaired glutamate uptake.

76

77   **Materials and Methods**

78   *Experimental animals*

79   Animals used in the experiments outlined below were approved for use by The University of

80   Sydney and University of Technology Sydney Animal Ethics Committees. Experiments were

4

81   performed under the guidelines of the Australian code of practice for the care and use of

82   animals for scientific purposes (National Health and Medical Research Council, Australia, 7th

83   Edition). In all experiments unless otherwise stated, 6 – 8 week old inbred C57bl/6 male

84   mice were used (91 in total). Animals were kept in 12hr light/dark cycles with food

85   (standard rodent chow) and water provided ad libitum.

86

87   *Induction and behavioural assessment of nerve injury*

88   Partial sciatic nerve ligation (PNL) was performed as described previously (Seltzer *et al.*

89   1990). Briefly, under isoflurane (Aerrane, Baxter) anaesthesia (2.5% in oxygen), the biceps

90   femoris muscle was blunt dissected to reveal the sciatic nerve proximal to its trifurcation.

91   Connective tissue surrounding the nerve was carefully removed to improve access. A spinal

92   hook was then used to lift the nerve without compression or stretching so that a single 6-0

93   silk suture could be threaded through approximately one-half of the nerve. This single

94   suture was tied tightly before returning the nerve to its original position. The musculature

95   was then sewn together with a single suture and the skin was brought together and closed

96   with cyanoacrylate glue (Vetbond™, 3M™).

97   The impact of nerve injury on hind paw weight bearing was assessed with a Linton

98   Incapacitance Tester (Linton Instrumentation, UK) prior to and 1, 4 and 7 days following

99   nerve injury (Strickland *et al.* 2008). Measurements were taken by averaging the

100   instantaneous force (measured as weight, in grams) applied to each hind-paw at pre-surgery

101   (baseline) and each day post-surgery. Each datum is the average of 4 measurements taken

102   at 10 second intervals. An incapacitance ratio was therefore derived as the force applied by

103   the injured hind paw / uninjured paw. Animals that failed to show a 25% or greater

104   reduction in their incapacitance ratio (7 of the 91 mice) were not used for biochemical or

105   electrophysiological experiments and were euthanized.

106   Immediately following incapacitance measurements, each animal was placed into a

107   plexiglass observation chamber (40cm x 20cm x 20cm) and was monitored for 5 min for

108   signs of spontaneous pain by scoring the number of events of hind-paw lifting, hind-paw

109   flicking or shaking, and hind paw tending. A composite score for each animal was calculated

110   by summing each score. As the mice were able to move freely about the enclosure, no

111   scoring bias was applied to the affected paw.

112

113   *Immunofluorescent detection of spinal glutamate transporters*

114   Following sodium pentobarbital administration, mice were transcardially perfused with 10

115   ml of a heparin containing (3000 IU /L) flush solution (in mM; 154 NaCl, 58.8 $NaNO_3$) before

116   perfusion with 100 ml of the fixation solution; 4% formaldehyde prepared in PBS (in mM;

117   25.3 $NaH_2PO_4.H_2O$, 108 Na_2HPO_4, 154 NaCl). Spinal cords were removed following fixation

118   and post-fixed for 1 hour, before transferring to 30% sucrose/PBS to cryoprotect the cords.

119   All steps used PBS as a buffer. Once sucrose had penetrated the cords (as determined by

120   cords sinking) they were snap-frozen in tissue support matrix (Tissue-Tek® O.C.T. compound,

121   Proscitech, Thuringowa, QLD, Australia) and stored at -80 ^{o}C until processed. Thirty

122   micrometer sections were then cut into PBS using a Leica cryostat (CM1850 UV) and stored

123   at 4 $^{\circ}$C. Only sections from the lumbar enlargement (L3 – L5) were used for staining.

124   For immunofluorescent staining, 6 sections from each of 4 mice per time point (or 4 naive

125   mice, 12 mice in total) were permeabilised in 0.3% Triton-X100/PBS (wash buffer) for 10

126   minutes before blocking with 10% normal horse serum (NHS; EAAT1-2) or goat serum (for

127   GFAP) for 30 minutes. Sections were then transferred into the appropriate primary antibody

128   diluted in wash buffer (EAAT1 1:4,000 Millipore; EAAT2 1:400 Millipore; EAAT3 1:1000

129   Millipore; GFAP 1:1,000 Abcam) and incubated overnight at room temperature with gentle

130   agitation. Excess primary antibody was removed with three 10 minutes washes of wash

131   buffer before a 2 hour incubation in secondary antibody (EAAT1/2; anti-guinea pig A488,

132   Jackson ImmunoResearch, GFAP; anti-rabbit A488, Invitrogen^{TM}, EAAT3; anti-mouse Cy3,

133   Jackson ImmunoResearch). Finally, sections were washed again with three 10 minutes

134   washes with wash buffer before mounting onto glass slides with fluoromount-G (Southern

135   Biotech, Alabama, USA). Digital images of individual sections were taken at 10X optical

136   magnification on an epifluorescent microscope. Densitometry was performed using ImageJ

137   software (National Institutes of Health, Bethesda USA). For high magnification of GFAP-

138   stained sections, 4 10X confocal images comprising 30 1μm z-sections were stitched

139   together using Photoshop® (Adobe, San Jose CA) to create one single image. Inlays are

140   comprised of 9, 60X confocal images comprising 30 1μm z-sections stitched together.

141

142   *In vitro electrophysiology*

7

143   Spinal cord slices (340 µm) from the lumbar enlargement L3-L5 (Rigaud *et al.* 2008) were

144   prepared from 24 nerve injured and 36 naive isoflurane anaesthetised mice on a Leica

145   VT1200S vibrating blade microtome (Leica Microsystems, North Ryde, Australia) in ice-cold

146   modified artificial cerebrospinal fluid (ACSF, in mM); choline chloride (120), glucose (11),

147    $NaHCO_3$ (25), KCl (2.5), NaH_2PO_4 (1.4), $CaCl_2$ (0.5), $MgCl_2$ (7), atropine (0.001). Slices were

148   allowed to recover for 1 hour at room temperature in ACSF (in mM); NaCl (125), KCl (2.5),

149   NaH_2PO_4 (1.25), $NaHCO_3$ (25), glucose (11), $MgCl_2$ (1.2), $CaCl_2$ (2.5) before being transferred

150   to a recording chamber where Dodt-contrast optics was used to identify lamina I/II

151   superficial dorsal horn neurons for patch-clamp electrophysiology. The internal solution of

152   the recording pipette contained (in mM); CsCl (140), EGTA (10), HEPES (5), $CaCl_2$ (2), MgATP

153   (2), NaGTP (0.3), QX314 chloride (5) and had an osmolality of 290 mOsm. Drugs were

154   superfused onto slices at a rate of 2 ml per minute in normal ACSF at a nominal 33^oC.

155   Whole-cell voltage clamp was performed using a Multiclamp 700B amplifier (Molecular

156   Devices, Sunnyvale CA) interfaced to an intel processor-based iMac computer (Apple,

157   Cupertino CA; Mac OS X 10.5) via an ITC-18 digitiser (Heka Elektronik, Ludwigshafen

158   Germany). Electrically-evoked EPSCs (eEPSCs) were elicited by stimulating dorsal roots

159   attached to the slice at 0.03Hz with bipolar tungsten electrodes so that an appropriately

160   sized current was produced in recorded neurons, in the range of 100 – 800 pA. eEPSCs were

161   sampled at 10 kHz and filtered at 4 kHz using Axograph X (Axograph Scientific, Australia).

162   AMPA receptor mediated currents were obtained by clamping the membrane potential at -

163   60 mV in the presence of picrotoxin (100 µM), strychnine (5 µM) and DL-AP5 (100 µM).

164   NMDA receptor mediated currents were obtained by clamping the membrane potential at

8

165   +40 mV in the presence of picrotoxin (100 μM), strychnine (5 μM) and CNQX (10 μM).

166   Miniature EPSCs were filtered (4 kHz low-pass filter) and sampled at 10 kHz for on-line and

167   later off-line analysis, and were recorded in the presence of picrotoxin (100 μM), strychnine

168   (5 μM) and tetrodotoxin (1 μM), to block GABAA, glycine and sodium channels, respectively.

169   Miniature EPSCs above a preset threshold (4 standard deviations above baseline noise) were

170   automatically detected by a sliding template algorithm, and then manually checked off-line.

171   Miniature EPSCs were then counted in 4 s epochs every 2 s to construct rate-time plots.

172   Data presented represent the average of at least 800 captured events over a minimum 5

173   minute interval for each condition (drug or vehicle) for each cell recorded (N = 4). Series

174   resistance (< 20 MΩ) was compensated by 70-80% in all patch-clamp experiments.

175   Recordings were stopped if series resistance deviated by more than 20% of baseline.

176

177   *Data analysis and statistics*

178   Densitometry of immunohistochemistry was performed using imageJ (National Institutes of

179   Health, Bethseda, USA). Behavioural testing was recorded by the observer in a notebook

180   before being manually entered into Prism (Version 5 for Windows, GraphPad Software Inc.

181   California, USA) for statistical analysis and generation of graphs. Illustrations were prepared

182   using Photoshop® CS4 and Illustrator® CS4 for Windows. Kinetics of AMPAR and NMDAR

183   evoked EPSCs were determined offline using the 'fit exponential' tool in Axograph on the

184   assembled average of 10 consecutive eEPSCs for each condition. The kinetics of

185   unperturbed (in the absence of uptake inhibitors) eEPSC decay were best described by a

186 single exponential. As with previous reports, the addition of a second exponential did not

187 improve the quality of the fit (Grosskreutz *et al.* 2003). Rise and decay kinetics for each

188 recording were only included for analysis if the assembled average trace was smooth

189 enough to confidently measure these parameters. The area under the curve was also

190 determined for each trace using Axograph. Statistical differences were determined using

191 one-way ANOVA with Dunn's multiple comparisons post-test (Western blots, behavioural

192 tests) and student's t-test (immunohistochemistry, electrophysiology) in Prism.

193 *Drugs*

194 Unless otherwise stated, all reagents were obtained from Sigma-Aldrich (St. Louis, Missouri,

195 USA). Disodium CNQX, picrotoxin, strychnine, DL-TBOA and DL-AP5 were purchased from

196 Tocris (Bristol, UK). Tetrodotoxin and QX314 chloride were obtained from Alamone Labs Ltd.

197 (Jerusalem, Israel).

198 **Results**

199

200 *Nerve injury-induced signs of neuropathic pain and astrocyte activation*

201 In agreement with previous reports, partial sciatic nerve ligation induced reliable signs of

202 pain (Seltzer *et al.* 1990) as well as increased staining of GFAP (Coyle 1998; Narita *et al.*

203 2006). From as early as 24 hours post-surgery, nerve injured mice displayed a significant

204 reduction in the force applied to the injured paw compared to baseline (Figure 1A. left/right

205 ratio, baseline = 1.08 ± 0.03 vs. Day 1 = 0.44 ± 0.02, P< 0.0001; ANOVA). This change

206 continued up to and beyond day 7 post-surgery (Day 4 = 0.51 ± 0.04, Day 7 = 0.58 ± 0.07, P<

207   0.0001; ANOVA). Similarly, signs of paw lifting, flicking and guarding remained elevated

208   during the 7 day post-surgical period (Figure 1B. Left vs. right Days 1, 4 and 7 P< 0.0001;

209   ANOVA). We examined the well established activation of astrocytes following PNL by

210   examining GFAP staining. As shown in Figure 1C the GFAP immunoreactivity was

211   significantly elevated after nerve injury with the greatest effect being observed 4 days post-

212   injury.

213

214   *Effect of PNL on expression of spinal glutamate transporters*

215   Following nerve injury, perfusion-fixed mouse spinal cord was sectioned for

216   immunohistochemical staining of glutamate transporters. Previous reports have indicated

217   that both glial and neuronal spinal glutamate transporter expression is perturbed by nerve

218   injury and inflammation (Harris *et al.* 1996; Sung *et al.* 2003; Wang *et al.* 2006; Wang *et al.*

219   2008; Xin *et al.* 2009).

220   Modest decreases in astrocytic glutamate transporter expression were observed in

221   immunohistochemically stained sections of lumbar spinal cord at days 4 and 7 post-injury.

222   The glial transporters, EAAT1 and EAAT2 (Figure 2A and B, resp.) showed small, persistent

223   decreases in ipsilateral expression when compared to contralateral dorsal horn. For EAAT1,

224   the approx. 7% decrease in optical density in the dorsal horn was not significant at either

225   day 4 or 7 after injury. However, when both post-injury days were pooled, the decrease was

226   significant (P < 0.05). For EAAT2, the 9% decreases in optical density for ipsilateral versus

227   contralateral dorsal horn were significantly reduced on both day 4 and day 7 after injury.

11

228   The small reduction in EAAT2 immunohistochemical staining was then further explored by

229   Western blot on crudely isolated dorsal horn soluble protein extracts in a separate group of

230   animals. In these experiments, no significant changes to total EAAT2 levels were found at

231   either post-injury time point (data not shown). As shown in figure 2D, no trends for changed

232   expression of EAAT3 were detected immunohistochemically. We should note however, that

233   the antibody used to detect EAAT3 was from the same species (mouse) as the experimental

234   animals and is most likely the cause of some non-specific staining, especially in the ventral

235   horn. However, in concurrent experiments performed without primary antibody (negative

236   controls), non-specific staining was not observed in the superficial dorsal horn where

237   analysis was performed (data not shown). Collectively, these data suggest that nerve injury

238   associated with development of neuropathic pain has only a modest impact on the

239   expression of glutamate transporters in the spinal dorsal horn.

240

241   *Effect of nerve injury on AMPAR synaptic current kinetics.*

242   If the small reduction in immunohistochemical staining for the astrocyte glutamate

243   transporters, EAAT1 and EAAT2, reflected reduced cell surface expression in the vicinity of

244   excitatory synapses, then this could lead to reduced extrasynaptic glutamate reuptake. If

245   this were to occur then kinetics of synaptic currents should be altered. We examined the

246   kinetics of AMPAR and NMDAR mediated eEPSCs 4 days after injury because maximal

247   effects on GFAP, as well as decreased expression of EAAT1 and EAAT2, were observed at

248   that time.

12

249   Example AMPAR- and NMDAR mediated eEPSCs are shown in figures 3A and 3B.

250   AMPAR and NMDAR eEPSC decay time constants were best fit by single exponentials as

251   previously described (Feldmeyer *et al.* 2002; Grosskreutz *et al.* 2003; Stubblefield and Benke

252   2010). Fitted time constants did not differ significantly for either the rise (naive; 0.95 ± 0.1

253   ms, N = 12, injured; 1.0 ± 0.15 ms, N = 10) or decay (naive; 6.15 ± 0.74 ms, N = 23, injured;

254   6.65 ± 0.95 ms, N = 20) of AMPAR-mediated eEPSCs in naive vs. injured animals, measured

255   in the presence of DL-AP5 (100 μM), picrotoxin (100 μM) and strychnine (5 μM). Similarly,

256   NMDAR rise time and decay kinetics, measured in the presence of CNQX (10 μM), picrotoxin

257   (100 μM) and strychnine (5 μM), were not affected by nerve injury (rise; naive; 6.29 ± 1.09

258   ms N = 8, injured; 6.63 ± 1.69 ms N = 6, decay; naive; 195.6 ± 24.18, N = 7, injured; 187.8 ±

259   28.82 N = 7). These findings suggest that impaired glutamate transporter activity might not

260   contribute greatly to primary afferent synaptic transmission after nerve injury.

261

262   *Effect of nerve injury on sensitivity of glutamate transporters to inhibition*

263   Measures of unperturbed decay time constants could be an insensitive measure of

264   reduced glutamate reuptake in the vicinity of synapses because decay kinetics of both

265   AMPAR and NMDAR mediated synaptic currents are dominated by channel kinetics rather

266   than glutamate reuptake (Dingledine *et al.* 1999). Such measures could also be confounded

267   by possible changes in subunit composition of AMPARs or NMDARs in pain states (Vikman *et*

268   *al.* 2008) although our data suggest that no such changes occur in mouse dorsal horn, 4 days

269   after nerve injury. Therefore, to further explore whether enhanced spillover of synaptic

270   glutamate develops after nerve injury, eEPSCs were recorded in the presence of a moderate

271   concentration of a non-specific glutamate transport inhibitor, DL-*threo*-β-Benzyloxyaspartic

272   acid (TBOA) (Shimamoto *et al.* 1998). By partially blocking glutamate reuptake to induce

273   detectable spillover from excitatory synapses, any pathologically enhanced spillover of

274   glutamate produced by nerve injury should be observed as an enhancement of these effects

275   as previously reported at other CNS synapses (Nie and Weng 2010). As expected in naive

276   animals, TBOA (30 and 100 µM) potentiated the duration but not amplitude of AMPAR

277   eEPSCs in a concentration dependent manner by introducing the appearance of a second,

278   late phase to the decay of the eEPSC without affecting the early decay phase (Figure 4A,B).

279   As shown in figure 4B, 100µM TBOA significantly increased the eEPSC late time constant (P =

280   0.015, from 36.5 ± 8.1 ms to 125.4 ± 20.4 ms, n = 6), as well as the area under the curve (P <

281   0.05, from 1688 ± 373 pA.ms to 6013 ± 1269 pA.ms, n = 6) in naive animals. Both measures

282   presumably reflect spillover of glutamate from subsynaptic to extrasynaptic sites and

283   adjacent synapses. In dorsal horn neurons from untreated animals, transporter inhibition

284   had no significant effect on the early decay time constant (control = 5.1 ± 0.5 ms, 30 µM =

285   5.6 ± 1.6 ms, 100 µM = 6.0 ± 1.2 ms), which is presumably dominated by decay kinetics of

286   channel opening (see also below).

287   In the presence of TBOA the addition of CNQX (10 µM in the continued presence of

288   DL-AP5, picrotoxin and strychnine) blocked all slow synaptic currents and nearly abolished

289   the fast component (n = 3). This suggests that the enhanced slow components of the eEPSC

290   induced by TBOA are mediated exclusively by AMPARs without any contribution from

291   mGluRs. mGluR-mediated slow eEPSCs have been reported in dorsal horn in the presence of

14

292   TBOA but only after high frequency stimulation of primary afferent fibres (Galik *et al.* 2008).

293   TBOA (100 μM but not 30 μM) also produced a small but significant inhibition of the

294   amplitude of eEPSCs (14 ± 1.8%), which could be mediated by spillover of glutamate to

295   presynaptic mGluR (Drew *et al.* 2008) or KA receptors (Perrais *et al.* 2010). A 30 μM

296   concentration of TBOA was therefore selected for subsequent experiments in nerve injured

297   tissue because it produced only a moderate enhancement of the eEPSC late decay time

298   constant without affecting amplitude.

299

300   If nerve injury does induce EAAT down-regulation in the vicinity of dorsal horn

301   primary afferent synapses, glutamate spillover might be enhanced by moderate EAAT

302   inhibition (30 μM TBOA) to a greater extent in nerve injured than control animals (Figure

303   3C). As shown in figure 3D, TBOA significantly increased the early decay time constant in

304   dorsal horn neurons from nerve injured animals, suggesting that transporters in close

305   proximity to glutamate release sites might be functionally modified to increase spillover.

306   Alternatively, nerve injured mice could express more extra-synaptic AMPA receptors in close

307   proximity to release sites. Nerve injury did not greatly influence distal extra-synaptic

308   receptor activation as no change to area under the curve, or late decay time constant was

309   observed following transporter inhibition. These findings suggest that reduced EAAT activity

310   in the vicinity of primary afferent synapses, if it occurs after nerve injury, is not due to a

311   widespread reduction in glutamate uptake capacity but is restricted to proximal

312   extrasynaptic sites.

313

314   To ensure that the enhancing effects of TBOA on AMPAR kinetics were not due to

315   presynaptic actions, miniature EPSCs (mEPSCs) were examined in naive animals. In the

316   presence of 1µM tetrodotoxin (TTX), no significant changes to mEPSC decay, amplitude or

317   frequency were observed during glutamate transporter inhibition in naive animals (100 µM

318   TBOA, N = 4) (Figure 5). This is consistent with the finding that the early decay time constant

319   of the eEPSC in uninjured mice was unaffected by TBOA and the expectation that mEPSCs,

320   being sporadic quantal events should produce little spillover to extrasynaptic AMPARs.

321

322   If reduced perisynaptic glutamate transporter activity does indeed explain the

323   increased early decay time constant of AMPAR-mediated synaptic events via increased

324   spillover, then it might also be possible to detect increased spillover to NMDA receptors. To

325   address this, we utilised the use-dependent NMDA receptor blocker (+)-MK-801 to block

326   subsynaptic NMDARs before enhancing glutamate spillover with TBOA, as reported at this

327   synapse (Nie and Weng 2009). In this experiment, stable baseline NMDAR-mediated eEPSCs

328   (in the presence of CNQX) for dorsal horn neurons in whole-cell voltage-clamp (+40mV)

329   were established by electrically stimulating the dorsal roots at 0.03Hz (Figure 6Ai). Then

330   active/open NDMARs were blocked during a ten minute superfusion of 50 µM MK-801. At

331   this time, subsynaptic NMDAR eEPSCs were completely blocked (Figure 6Aii). A ten minute

332   wash was then performed to remove unbound MK-801 whilst stimulation continued (Figure

333   6Aii). Following this, 100µM TBOA was superfused onto slices to generate glutamate

16

334   spillover (Figure 6Aiii). As shown in figure 6A, this approach successfully induced glutamate

335   spillover and activation of extra-synaptic NMDARs. When performed in slices from nerve

336   injured mice, no change in time to peak was observed (Figure 6B). However a small non-

337   significant trend for increase in peak amplitude and area under the curve were observed.

338   Collectively however, these findings suggest that no significant increase of spillover to extra-

339   synaptic NMDA receptors takes place following nerve injury. However, this does not rule out

340   the possibility of increased spillover combined with reduced NMDAR expression.

341

342   **Discussion**

343   The present study suggests that nerve injury associated with allodynia and astroglial

344   activation produces only small changes to expression and function of glutamate

345   transporters in the vicinity of primary afferent synapses. Our findings therefore argue

346   against a major role for a contribution of glutamate transporter dysfunction and glutamate

347   spillover in the development of neuropathic pain. It is well established that peripheral nerve

348   injury leads to changes in the expression and function of markers of glutamatergic

349   neurotransmission in the spinal dorsal horn. These changes are also thought to be

350   responsible, in part, for the development and maintenance of neuropathic pain (Tsuda *et al.*

351   2005; Sandkuhler 2007; Scholz and Woolf 2007; Vikman *et al.* 2008). One of the ways in

352   which this has been proposed to occur is a generalized down-regulation of glutamate

353   transporters in the vicinity of synapses and a concomitant increase in the expression and

354   function of glutamate receptors (Harris *et al.* 1996; Popratiloff *et al.* 1998; Garry *et al.* 2003;

355   Sung *et al.* 2003; Yang *et al.* 2004; Wang *et al.* 2006; Sung *et al.* 2007; Tawfik *et al.* 2008;

17

356   Wang *et al.* 2008). For example, in rats, PNL induced an approximately 51% and 40%

357   reduction in EAAT1 (Xin *et al.* 2009) and EAAT2 (Maeda *et al.* 2008; Xin *et al.* 2009),

358   respectively, expression at day 7. In another model of neuropathic pain, chronic constriction

359   injury (CCI), these losses are preceded by an increase in EAAT1-3 at day 4 (Sung *et al.* 2003;

360   Wang *et al.* 2006). However, despite an overall increase in total protein at this time,

361   glutamate reuptake activity was in fact lower than in sham-operated animals (Sung *et al.*

362   2003). In contrast to the studies above, we found that nerve injury resulted in modest

363   decreases in expression over the same 4-7 day period. When we looked at EAAT2 expression

364   further by Western blot, these reductions were lost. This may be due to transporter

365   redistribution in astrocytes, exposing changes in epitope availability in

366   immunohistochemical studies. It is hard to reconcile the differences in EAAT expression

367   observed between ours and previous studies. Others have reported increased expression of

368   all three transporters up to 4 days after chronic constriction injury in rats (Sung et al., 2003)

369   but decreased expression after 7 days (Sung et al., 2003; Wang et al. 2006). Explanations

370   could be that of species differences, as our experiments were performed in mice and not

371   rat, or models used (partial nerve ligation versus chronic constriction injury). For example, in

372   mice mechanical allodynia and expression changes of nociceptive markers (e.g. NK1) are

373   typically restricted to the ipsilateral hind paw (Malmberg and Basbaum 1998), whereas in

374   rat, these changes are bilateral. It has been shown previously partial nerve ligation and

375   chronic constriction models induce contrasting phenotypes of hot and cold hyperalgesia as

376   well as mechanical allodynia (Bennett and Xie 1988; Seltzer *et al.* 1990). These adaptations

377   were thought to create conditions whereby synaptic glutamate has the potential to both

18

378   persist within the synapse but also to diffuse out of the synapse to bind extra-synaptic

379   receptors thereby enhancing primary afferent synaptic transmission and plasticity.

380

381   To test whether or not this occurs at functioning synapses, we made use of the

382   broad-spectrum glutamate transport inhibitor TBOA to drive moderately increased

383   glutamate spillover in the spinal dorsal horn. By inhibiting all three transporters with 100

384   µM TBOA, a substantial late phase decay time constant for AMPARs was produced.

385   Furthermore, the area under the curve of the AMPAR current (current density) increased

386   from 249% in 30 µM TBOA to 384 % of control in 100 µM TBOA, suggesting a significant role

387   for EAAT1 and EAAT2 in glutamate reuptake in the dorsal horn. Due to the rapid

388   desensitization of AMPARs following agonist binding, the facilitation of the synaptic current

389   under these conditions is likely due to diffusion of synaptically released glutamate to

390   proximal (early time constant) extra-synaptic AMPARs and more remote extrasynaptic

391   receptors and synapses (Beurrier *et al.* 2009).

392

393   If nerve-injury results in a basal increase in synaptic and perisynaptic glutamate

394   concentrations, then eEPSCs from nerve-injured mice should display slower decay kinetics

395   than naïve mice, similar to that observed for TBOA-induced spillover. In the absence of

396   TBOA, decay time constants did not differ between naive and nerve injured mice suggesting

397   AMPAR composition in the vicinity of synapses is not greatly altered and spillover, if present,

398   is modest. Interestingly, nerve injury was associated with an increased early decay time

399   constant of AMPARs, suggesting increased peri-synaptic glutamate spillover or,

400   alternatively, increased perisynaptic AMPAR density.

401

402   This increased early decay time constant after nerve injury in the presence of TBOA

403   (30 µM) does not appear to be due simply to increased sensitivity to TBOA. Firstly, the late

404   decay time constant was unaffected after nerve injury in this concentration of TBOA but was

405   greatly enhanced in control tissue by a higher concentration of TBOA (100 µM). Secondly,

406   the early decay time constant was completely unaffected by the higher concentration of

407   TBOA (100 µM) in control spinal cord. These findings strongly suggest the increased early

408   decay time constant observed in TBOA reflects either an increased density of extrasynaptic

409   AMPARs that are silent in the absence of transporter inhibition or, alternatively impaired

410   transporter (EAAT1 and/or EAAT2) activity in close proximity to synapses that enhances

411   sensitivity to TBOA.

412   In a similar study in rats by Nie and Weng (2010), an EAAT2-specific blocker,

413   dihydrokainate (DHK), significantly increased NMDAR EPSC amplitude, latency, duration and

414   decay time in naive rats, but failed to elicit any response in nerve injured rats, suggesting

415   complete loss of EAAT2 function despite expression levels of around 40% compared to

416   controls. This finding is hard to reconcile with our results. However it should be noted that

417   these experiments were performed at 8-14 days post-injury in rats, whereas our

418   electrophysiological recordings were made at day 4 post-injury in mice.

419

420   The possibility that perisynaptic spillover is increased can also be tested by

421   examining the effect of TBOA on NMDARs after blockade of active subsynaptic receptors

422   with MK-801. In this case there was no significant difference to the degree of extra-synaptic

423   NMDAR activation at primary afferent synapses from nerve injured animals. This

424   experiment therefore failed to confirm the interpretation that the increased early decay

425   time constants induced by TBOA in nerve injured animals was due to increased perisynaptic

426   glutamate spillover. There was, however, a non-significant trend for increased peak

427   amplitude of the extrasynaptic NMDAR-mediated eEPSC which is consistent with a small

428   increase in spillover. There are other potential explanations for the discrepancy between

429   the AMPAR and NMDAR-mediated results. It is possible that the increased early decay time

430   constant of the AMPAR-mediated eEPSC in the presence of TBOA reflects spillover to very

431   proximal extrasynaptic AMPARs or there may be an increase in extrasynaptic AMPAR

432   density following nerve injury rather than increased spillover per se. There is evidence for

433   AMPAR subunit adaptations during inflammatory pain that could be associated with

434   extrasynaptic insertion of AMPARs (Tao 2010) but whether or not similar adaptations

435   develop in nerve injury-induced pain is unknown. It is also possible that spillover to

436   extrasynaptic NMDARs in the presence of TBOA (100 μM) is mediated more by receptors

437   more distal to release sites than the AMPARs contributing to the early decay phase

438   enhanced by nerve injury. If so, measured NMDAR spillover may be similar to the late decay

439   phase of the AMPAR-mediated eEPSC in the presence of TBOA that is unaffected by nerve

440   injury.

441

442   In conclusion, the present study suggests that peripheral nerve injury at a time

443   associated with neuropathic pain and astrocyte activation does not greatly influence the

444   expression of astrocytic glutamate transporters in the superficial dorsal horn, nor does it

445   produce substantial extrasynaptic spillover of glutamate from primary afferent synapses.

446   However, in the close vicinity of synapses, glutamate transporter function may be prone to

447   ineffective uptake under extreme circumstances and lead to enhanced receptor activation.

448

449   **Acknowledgements**

452

Figure legends

454   Figure 1. Effect of nerve injury on the development of neuropathic pain. A) Hind paw

455   incapacitance test revealing significant weight shift from left (injured) to right hind paw.

456   Numbers in columns represent number of animals tested. B) PNL produces significant

457   increase in the rate of spontaneous behaviours indicative of neuropathic pain. C) GFAP

458   immunoreactivity in a spinal cord section from a nerve injured mouse (inj =

459   injured/ipsilateral) and histogram revealing significant increase in GFAP densitometry at day

460   4 post-injury (N = 4 in each group).

461

462   Figure 2. Effect of nerve injury on expression of spinal glutamate transporters.

463   Immunohistochemistry of glutamate transporters EAAT1 (A), EAAT2 (B) and EAAT3 (C)

464   following nerve injury reveals significant reduction of EAAT1 and EAAT2 between 4 and 7

465   days (* = P < 0.05, inj = injured/ipsilateral side, N = 4 in each group).

466

467   Figure 3. Effect of nerve injury on the kinetics of AMPAR and NMDAR-mediated eEPSCs.

468   Example synaptic current traces from eEPSCs mediated by AMPAR (A) and NMDAR (B)

469   reveal no significant change to rise or decay kinetics observed after nerve injury.

470

471   Figure 4. Effect of glutamate transporter inhibition on eEPSCs. A) Representative AMPAR

472   eEPSC showing effect of 30uM TBOA. Thin red lines depict fitted exponentials for early and

473   late components of decay. B) Effects of 30 µM and 100 µM TBOA on parameters of AMPAR

474   eEPSCs in dorsal horn neurons from naive mice expressed as percentage of pre-TBOA

475   baseline. C) Representative current traces of naive vs. nerve injured mice AMPAR eEPSCs in

476   the presence of TBOA (30 µM) compared to baseline. D) The effect of 30 µM TBOA on eEPSC

477   amplitude, decay kinetics and AUC in naive vs. nerve injured mice (percentage increase; * =

478    $P < 0.05$, numbers within histograms represent number of cells; N).

479

480   Figure 5. Effect of TBOA on miniature EPSCs. A) Representative recording of mEPSC events

481   before (CONTROL) and during application of TBOA. Enlarged is a single captured event from

482   a baseline recording. B) Representative mEPSC traces from averaged events in the presence

483   of TBOA. The histogram on the right reveals no deviation from baseline for decay,

484   amplitude, or rate, are observed in the presence of TBOA (N = 4). C) Cumulative probability

485   plots for current amplitude and rate in the presence of TBOA.

486

487   Figure 6. Effect of nerve injury on glutamate spillover to peri-synaptic NMDARs. A) Example

488   NMDAR current traces from a from a single dorsal horn neuron at baseline (i), following

489   washout of MK-801 (ii), and then after superfusion of TBOA (iii). Current traces are overlaid

490   for comparison in (iv). B) Effect of nerve injury on kinetics of peri-synaptic NMDARs in

491   presence of TBOA following sub-synaptic NMDAR blockade with MK-801. Numbers within

492   histogram represent numbers of cells (N).

493   References

Bennett, G. J. and Y. K. Xie (1988). "A peripheral mononeuropathy in rat that produces disorders of pain sensation like those seen in man." Pain **33**(1): 87-107.

Beurrier, C., G. Bonvento, *et al.* (2009). "Role of glutamate transporters in corticostriatal synaptic transmission." Neuroscience **158**(4): 1608-1615.

Chaudhry, F. A., K. P. Lehre, *et al.* (1995). "Glutamate transporters in glial plasma membranes: highly differentiated localizations revealed by quantitative ultrastructural immunocytochemistry." Neuron **15**(3): 711-720.

Coyle, D. E. (1998). "Partial peripheral nerve injury leads to activation of astroglia and microglia which parallels the development of allodynic behavior." Glia **23**(1): 75-83.

Danbolt, N. C. (2001). "Glutamate uptake." Prog Neurobiol **65**(1): 1-105.

Dingledine, R., K. Borges, *et al.* (1999). "The glutamate receptor ion channels." Pharmacol Rev **51**(1): 7-61.

Drew, G. M., V. A. Mitchell, *et al.* (2008). "Glutamate spillover modulates GABAergic synaptic transmission in the rat midbrain periaqueductal grey via metabotropic glutamate receptors and endocannabinoid signaling." J Neurosci **28**(4): 808-815.

Feldmeyer, D., J. Lubke, *et al.* (2002). "Synaptic connections between layer 4 spiny neurone-layer 2/3 pyramidal cell pairs in juvenile rat barrel cortex: physiology and anatomy of interlaminar signalling within a cortical column." J Physiol **538**(Pt 3): 803-822.

Galik, J., D. H. Youn, *et al.* (2008). "Involvement of group I metabotropic glutamate receptors and glutamate transporters in the slow excitatory synaptic transmission in the spinal cord dorsal horn." Neuroscience **154**(4): 1372-1387.

Garry, E. M., A. Moss, *et al.* (2003). "Specific involvement in neuropathic pain of AMPA receptors and adapter proteins for the GluR2 subunit." Mol Cell Neurosci **24**(1): 10-22.

Graham, B. A., A. M. Brichta, *et al.* (2007). "Moving from an averaged to specific view of spinal cord pain processing circuits." J Neurophysiol **98**(3): 1057-1063.

Grosskreutz, J., A. Zoerner, *et al.* (2003). "Kinetic properties of human AMPA-type glutamate receptors expressed in HEK293 cells." Eur J Neurosci **17**(6): 1173-1178.

Harris, J. A., M. Corsi, *et al.* (1996). "Upregulation of spinal glutamate receptors in chronic pain." Neuroscience **74**(1): 7-12.

25

533 Liaw, W. J., R. L. Stephens, Jr*., et al.* (2005). "Spinal glutamate uptake is
534   critical for maintaining normal sensory transmission in rat spinal
535   cord." <u>Pain</u> **115**(1-2): 60-70.
536 Maeda, S., A. Kawamoto*, et al.* (2008). "Gene transfer of GLT-1, a glial
537   glutamate transporter, into the spinal cord by recombinant
538   adenovirus attenuates inflammatory and neuropathic pain in rats."
539   <u>Mol Pain</u> **4**: 65.
540 Malmberg, A. B. and A. I. Basbaum (1998). "Partial sciatic nerve injury in
541   the mouse as a model of neuropathic pain: behavioral and
542   neuroanatomical correlates." <u>Pain</u> **76**(1-2): 215-222.
543 Narita, M., T. Yoshida*, et al.* (2006). "Direct evidence for spinal cord
544   microglia in the development of a neuropathic pain-like state in
545   mice." <u>J Neurochem</u> **97**(5): 1337-1348.
546 Nie, H. and H. R. Weng (2009). "Glutamate transporters prevent excessive
547   activation of NMDA receptors and extrasynaptic glutamate spillover
548   in the spinal dorsal horn." <u>J Neurophysiol</u> **101**(4): 2041-2051.
549 Nie, H. and H. R. Weng (2010). "Impaired glial glutamate uptake induces
550   extrasynaptic glutamate spillover in the spinal sensory synapses of
551   neuropathic rats." <u>J Neurophysiol</u> **103**(5): 2570-2580.
552 Peghini, P., J. Janzen*, et al.* (1997). "Glutamate transporter EAAC-1-deficient
553   mice develop dicarboxylic aminoaciduria and behavioral
554   abnormalities but no neurodegeneration." <u>EMBO J</u> **16**(13): 3822-
555   3832.
556 Perrais, D., J. Veran*, et al.* (2010). "Gating and permeation of kainate
557   receptors: differences unveiled." <u>Trends Pharmacol Sci</u> **31**(11): 516-
558   522.
559 Popratiloff, A., R. J. Weinberg*, et al.* (1998). "AMPA receptors at primary
560   afferent synapses in substantia gelatinosa after sciatic nerve section."
561   <u>Eur J Neurosci</u> **10**(10): 3220-3230.
562 Rigaud, M., G. Gemes*, et al.* (2008). "Species and strain differences in rodent
563   sciatic nerve anatomy: implications for studies of neuropathic pain."
564   <u>Pain</u> **136**(1-2): 188-201.
565 Rothstein, J. D., M. Dykes-Hoberg*, et al.* (1996). "Knockout of glutamate
566   transporters reveals a major role for astroglial transport in
567   excitotoxicity and clearance of glutamate." <u>Neuron</u> **16**(3): 675-686.
568 Rothstein, J. D., L. Martin*, et al.* (1994). "Localization of neuronal and glial
569   glutamate transporters." <u>Neuron</u> **13**(3): 713-725.
570 Sandkuhler, J. (2007). "Understanding LTP in pain pathways." <u>Mol Pain</u> **3**:
571   9.

572   Scholz, J. and C. J. Woolf (2007). "The neuropathic pain triad: neurons,
573   immune cells and glia." <u>Nat Neurosci</u> **10**(11): 1361-1368.
574   Seltzer, Z., R. Dubner, *et al.* (1990). "A novel behavioral model of
575   neuropathic pain disorders produced in rats by partial sciatic nerve
576   injury." <u>Pain</u> **43**(2): 205-218.
577   Shimamoto, K., B. Lebrun, *et al.* (1998). "DL-threo-beta-benzyloxyaspartate,
578   a potent blocker of excitatory amino acid transporters." <u>Mol</u>
579   <u>Pharmacol</u> **53**(2): 195-201.
580   Stoffel, W., R. Korner, *et al.* (2004). "Functional analysis of glutamate
581   transporters in excitatory synaptic transmission of GLAST1 and
582   GLAST1/EAAC1 deficient mice." <u>Brain Res Mol Brain Res</u> **128**(2):
583   170-181.
584   Strickland, I. T., J. C. Martindale, *et al.* (2008). "Changes in the expression of
585   NaV1.7, NaV1.8 and NaV1.9 in a distinct population of dorsal root
586   ganglia innervating the rat knee joint in a model of chronic
587   inflammatory joint pain." <u>Eur J Pain</u> **12**(5): 564-572.
588   Stubblefield, E. A. and T. A. Benke (2010). "Distinct AMPA-type
589   glutamatergic synapses in developing rat CA1 hippocampus." <u>J</u>
590   <u>Neurophysiol</u> **104**(4): 1899-1912.
591   Sun, W., K. M. Hoffman, *et al.* (2011). "Specificity and Actions of an
592   Arylaspartate Inhibitor of Glutamate Transport at the Schaffer
593   Collateral-CA1 Pyramidal Cell Synapse." <u>PLoS One</u> **6**(8): e23765.
594   Sung, B., G. Lim, *et al.* (2003). "Altered expression and uptake activity of
595   spinal glutamate transporters after nerve injury contribute to the
596   pathogenesis of neuropathic pain in rats." <u>J Neurosci</u> **23**(7): 2899-
597   2910.
598   Sung, B., S. Wang, *et al.* (2007). "Altered spinal arachidonic acid turnover
599   after peripheral nerve injury regulates regional glutamate
600   concentration and neuropathic pain behaviors in rats." <u>Pain</u> **131**(1-
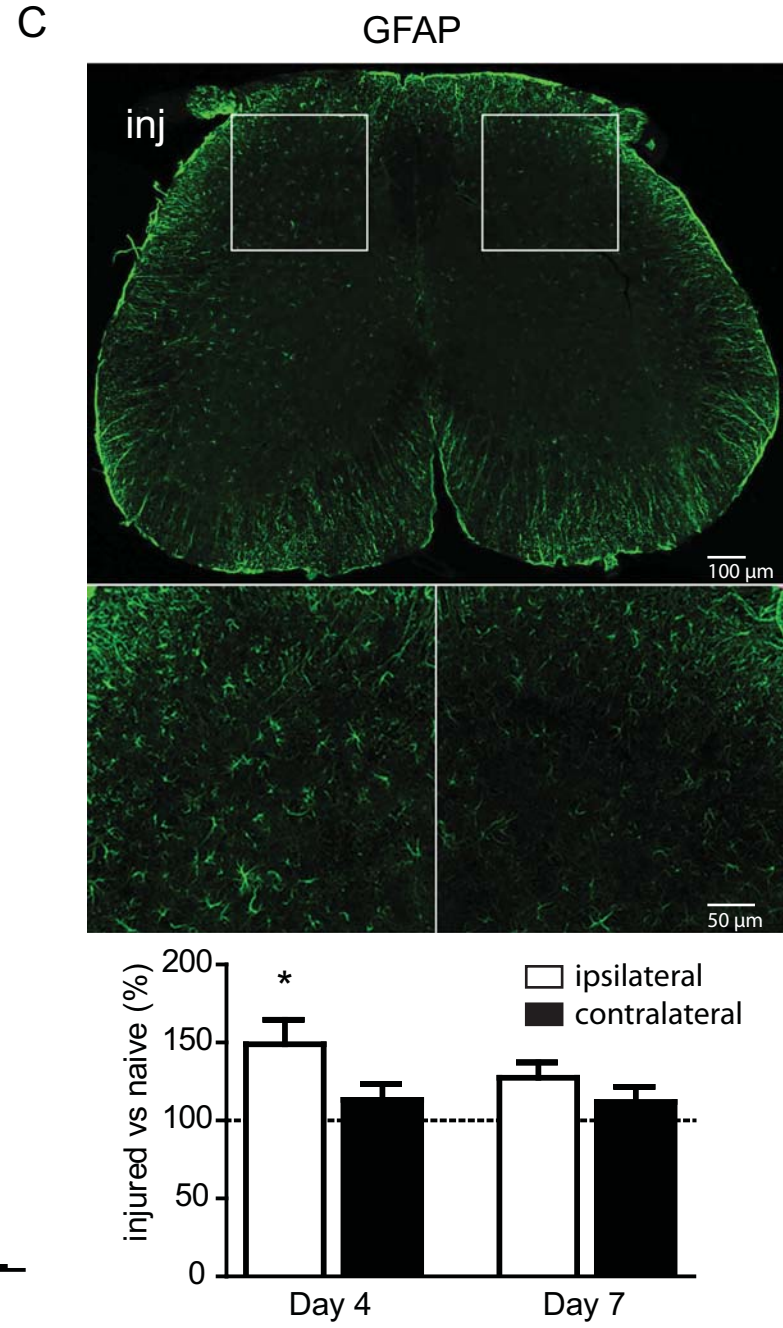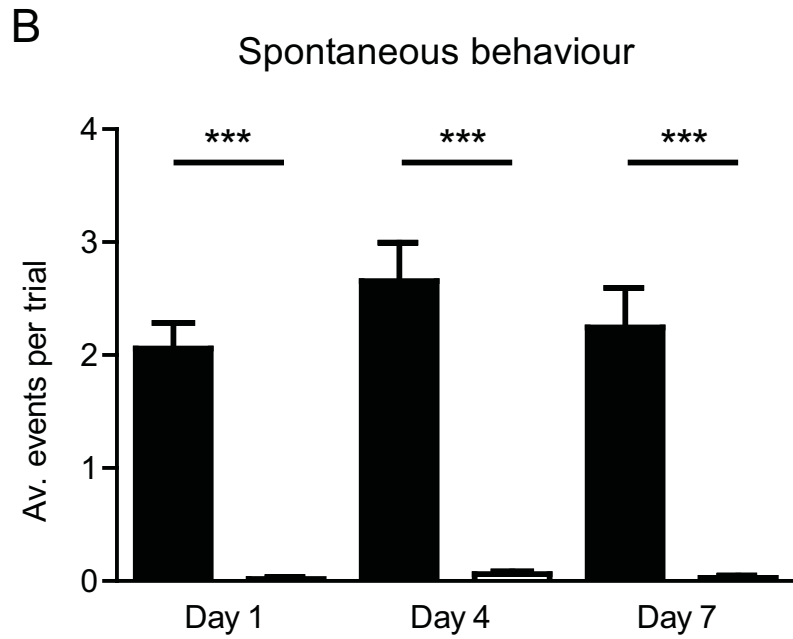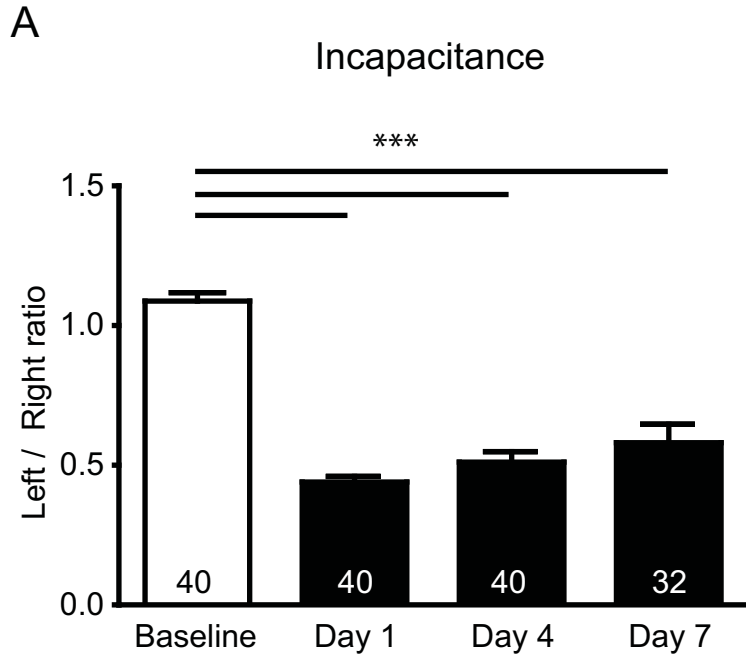601   2): 121-131.
602   Tao, Y. X. (2010). "Dorsal horn alpha-amino-3-hydroxy-5-methyl-4-
603   isoxazolepropionic acid receptor trafficking in inflammatory pain."
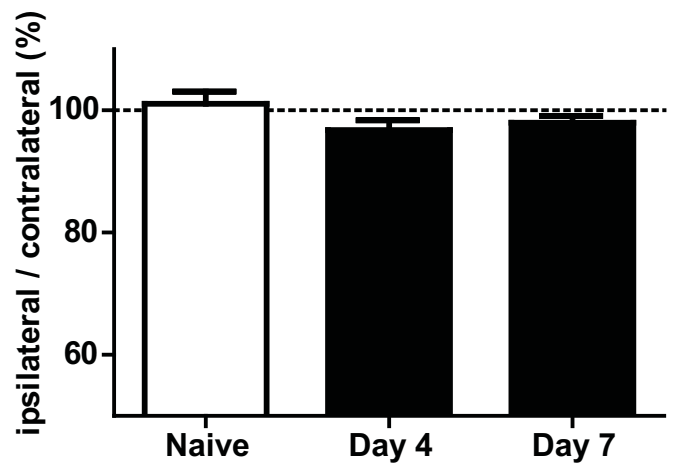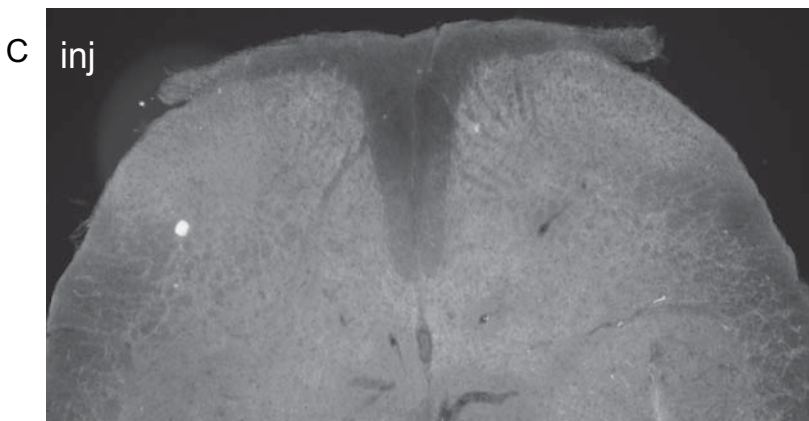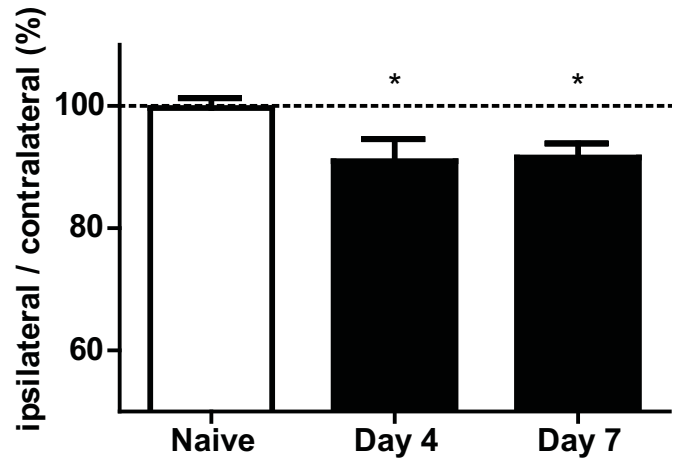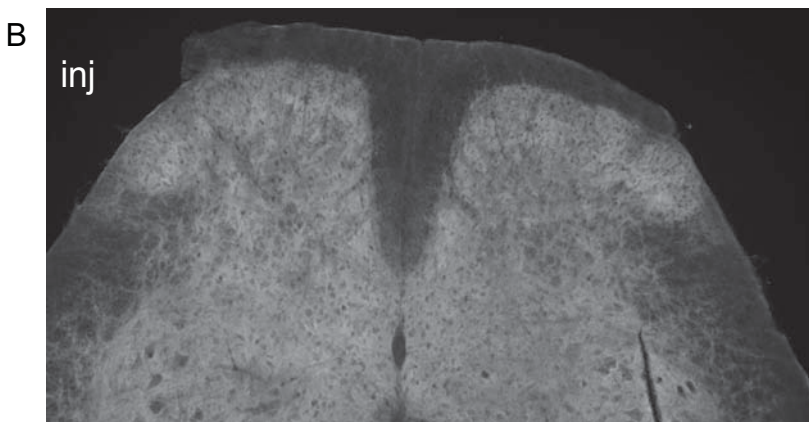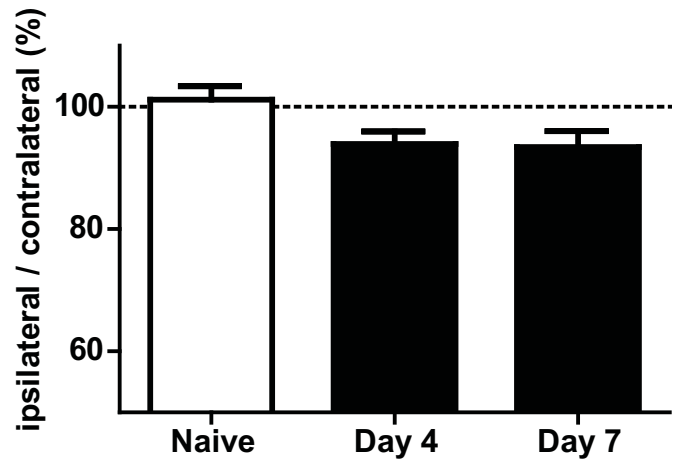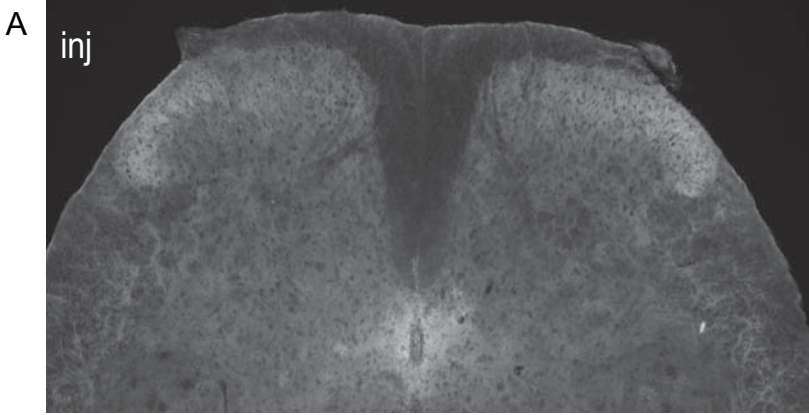604   <u>Anesthesiology</u> **112**(5): 1259-1265.
605   Tawfik, V. L., M. R. Regan, *et al.* (2008). "Propentofylline-induced astrocyte
606   modulation leads to alterations in glial glutamate promoter
607   activation following spinal nerve transection." <u>Neuroscience</u> **152**(4):
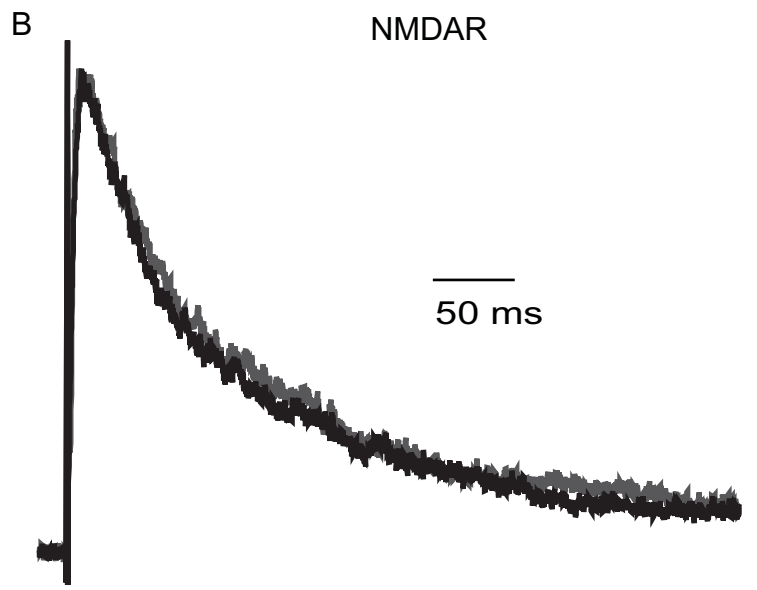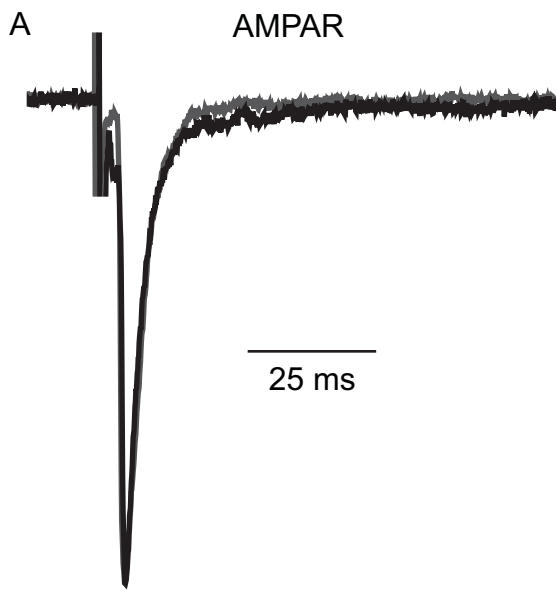608   1086-1092.

609 Tsuda, M., K. Inoue, *et al.* (2005). "Neuropathic pain and spinal microglia: a
610   big problem from molecules in "small" glia." <u>Trends Neurosci</u> **28**(2):
611   101-107.
612 Vikman, K. S., B. K. Rycroft, *et al.* (2008). "Switch to Ca2+-permeable AMPA
613   and reduced NR2B NMDA receptor-mediated neurotransmission at
614   dorsal horn nociceptive synapses during inflammatory pain in the
615   rat." <u>J Physiol</u> **586**(2): 515-527.
616 Wang, S., G. Lim, *et al.* (2006). "Downregulation of spinal glutamate
617   transporter EAAC1 following nerve injury is regulated by central
618   glucocorticoid receptors in rats." <u>Pain</u> **120**(1-2): 78-85.
619 Wang, W., Y. Wang, *et al.* (2008). "Temporal changes of astrocyte activation
620   and glutamate transporter-1 expression in the spinal cord after
621   spinal nerve ligation-induced neuropathic pain." <u>Anat Rec (Hoboken)</u>
622   **291**(5): 513-518.
623 Weng, H. R., J. H. Chen, *et al.* (2006). "Inhibition of glutamate uptake in the
624   spinal cord induces hyperalgesia and increased responses of spinal
625   dorsal horn neurons to peripheral afferent stimulation."
626   <u>Neuroscience</u> **138**(4): 1351-1360.
627 Xin, W. J., H. R. Weng, *et al.* (2009). "Plasticity in expression of the glutamate
628   transporters GLT-1 and GLAST in spinal dorsal horn glial cells
629   following partial sciatic nerve ligation." <u>Mol Pain</u> **5**: 15.
630 Yang, L., F. X. Zhang, *et al.* (2004). "Peripheral nerve injury induces trans-
631   synaptic modification of channels, receptors and signal pathways in
632   rat dorsal spinal cord." <u>Eur J Neurosci</u> **19**(4): 871-883.

633

634

A **Incapacitance**

***

Left / Right ratio

Baseline   Day 1   Day 4   Day 7
40   40   40   32

B **Spontaneous behaviour**

***   ***   ***

Av. events per trial

Day 1   Day 4   Day 7

C **GFAP**

inj

100 μm

50 μm

injured vs naive (%)

*

□ ipsilateral
■ contralateral

Day 4   Day 7

A

inj

B

inj

C

inj

A AMPAR

B NMDAR

25 ms

50 ms

Naive   Injured

A

Naive

50 pA

50 ms

■ control
■ TBOA 30 μM
━ fitted exponents

B

% of baseline

Ampl.   τ$_{early}$ τ$_{late}$ AUC

□ 30 μM   ■ 100 μM

C

Naive vs Injured

50 ms

━ Naive
━ Naive + TBOA
━ Injured
━ Injured + TBOA

D

Ampl.   τ$_{early}$ τ$_{late}$ AUC

□ Naive   ■ Injured

A

CONTROL

100 μM TBOA

10 pA
1 s

B

CONTROL   100 μM TBOA

150

% of baseline

100

50

0

Decay   Amplitude   Rate

C

Cumulative Probability

1

0.5

0

10   20   30   40   50
Current (pA)

30   60
Rate (s^{-1})

A

i

ii

50 pA

100 ms

1. NMDAR eEPSC   2. MK-801 washout

iii

iv

3. TBOA superfusion   4. Overlay

B

Peak Ampl.   TtP   AUC

□ Naive   ■ Injured